Available online at www.sciencedirect.com
ScienceDirect
Comput. Methods Appl. Mech. Engrg. 386 (2021) 114126
Computer methods in applied mechanics and engineering
www.elsevier.com/locate/cma

Efficient multi-frequency solutions of FE–BE coupled structural–acoustic problems using Arnoldi-based dimension reduction approach

Xiang Xie*, Yijun Liu

Department of Mechanics and Aerospace Engineering, Southern University of Science and Technology, Shenzhen, 518055, China

Received 18 December 2020; received in revised form 10 May 2021; accepted 13 August 2021
Available online 5 September 2021

Abstract

The frequency sweep analysis is indispensable for the performance prediction and optimization design of structural–acoustic interaction problems. The coupled finite element and boundary element (FE–BE) method has been widely used to perform such simulations. However, the straightforward solution of the resulting hybrid model for a large number of frequencies is computationally prohibitive due to the unfavorable properties of involved matrices, e.g. large-scale, non-symmetric and especially frequency-dependent. In order to ease this challenge, a three-step structure-preserving model order reduction method is presented, which is based on an offline-online computing framework. As a first step, the second-order Arnoldi process is used to speed up calculations of the sparse structural part of the strongly coupled system. In a second step, the low-dimensional approximations of the FE unknown variables are eliminated from the global system of equations and after that the remaining dense BE degrees of freedom are reduced by application of the standard Arnoldi-based Krylov subspace algorithm. A transformation technique based on Taylor's theorem is incorporated to decouple the frequency from the Green's function and a column-by-column low-memory projection is further sought to favor the overall storage requirements. In the last step, a robust reduced order model can be quickly retrieved by simple algebraic manipulations, which allows a direct solver without any costly matrix operation to be used for the online sweeps, requiring only a very small fraction of the total CPU runtime. Two numerical cases are investigated to highlight the potential of the proposed approach in multi-frequency applications.

Keywords: Vibro-acoustics; Model order reduction; FE–BE coupling; Fast direct solver; Frequency sweep

1. Introduction

Control of excessive noise and structural vibration is a growing concern for protecting human health and machinery equipments from exposure to unwanted operational forces and environmental noise originating from numerous sources: transportation, wind turbine and so on. Such trend and ever tightening regulations/targets have driven designers and manufacturers in many industries to evaluate the dynamic and acoustic qualities and especially the structural–acoustic coupling characteristics of their (lightweight) products and services, which is crucial for the

* Corresponding author.
E-mail address: xiex@sustech.edu.cn (X. Xie).

https://doi.org/10.1016/j.cma.2021.114126

desired vibration insulation and low-noise high-quality design and optimization. In order to decrease the time-to-market, Computer Aided Engineering (CAE) techniques play a significant role in the modern integrated design stage by the use of virtual computational prototypes to replace the experimental physical ones, i.e. from *a posteriori* to *a priori* analysis. During the past decades, notable progress has been made in the development and validation of numerical tools for accurate prediction of dynamic characteristics of increasingly complex three-dimensional (3D) engineering systems. Among the various classical CAE computational methodologies, the finite element method (FEM) [1] is widely used to obtain detailed information on the performance of vibrating structures or purely interior acoustics or coupled structural acoustics in bounded domains with arbitrarily complex shape, boundary conditions and material behaviors, while the boundary element method (BEM) [2] has natural strengths in handling acoustic radiation/scattering problems in infinite medium. Therefore, in order to exploit the advantages of both methods, the classical FE–BE coupling method [3–11] is favored to solve exterior fluid–structure interaction problems, e.g. sound radiation of submarines, design of loudspeakers, in which different coupling formulations in terms of both conforming meshes [9] and non-conforming cases [8,10] have been extensively discussed.

The use of hybrid FE–BE solution framework, however, often results in high-dimensional, non-symmetric and frequency-dependent computational models, which makes the original system-level full-scale simulations very time consuming and memory demanding. In order to improve the efficiency of modal analyses of structural–acoustic coupling problems, the Lanczos algorithm [12], Krylov–Schur solver [13], modal decomposition [14], contour integral method [15–17] and resolvent sampling based Rayleigh–Ritz method [18] have been employed to compute the related nonlinear eigenvalue problem.

In addition, evaluating response function over a wide frequency range with densely sampled step is often necessary to observe the level of vibration and noise emission and to assess the influence of passive/active strategies in structural dynamics and noise control engineering. In this instance, for frequency sweep analyses all the entries in the system matrices of BE part have to be continually recalculated and then the established global coupling model has to be resolved multiple times, which increase the computational complexity heavily as compared to the numerical eigenanalysis. Therefore, the performance prediction of large-scale exterior vibro-acoustic dynamical models is still challenging.

In order to alleviate these downsides, a variety of fast calculation schemes have been developed in the context of fully coupled FE–BE analyses. In particular, model order reduction (MOR) techniques are of intense interest to construct an orthonormal basis spanning a low-dimensional subspace onto which the original full-order model (FOM) is projected to obtain a reliable reduced-order model (ROM). Different approaches differ in how the projection basis is constructed. For the structural FE submodel, the Krylov subspace as the projection subspace has been used to reduce the displacement degrees of freedom (DOFs), whereas the acoustic BE submodel is left unchanged [19]. In fact, most of reduced-order modeling methods, e.g. the first-order Arnoldi (FOAR) method [20,21] for linear dynamical systems, the second-order Arnoldi (SOAR) method [22,23] for second-order problems and of course, the traditional modal superposition method [24] can be directly applied to the structural part without any difficulty due to its sparse and frequency-independent properties. Details concerning the comparison and assessment of existing low-order approximation approaches for structural dynamics analyses modeled using FEM are reviewed; see e.g. [25–27] and references therein. Among those, an important open question is how to determine the optimal order of a reduced system with satisfactory accuracy for practical use, preferably in an automatic manner. Since a complete reference solution, e.g. the exact solution is not known beforehand, the strategies proposed in the literature are often based on the relative input/output residual [20,28,29] or the difference between two reduced-order models [20,30–32] to estimate the true error such that the evaluation of the (computationally expensive) FOM can be avoided.

Compared with the FE submatrices, the dimension of the BE submatrices in the global system of equations is usually much smaller, especially for models with complicated internal setups, e.g. in the presence of reinforcement treatments including ring stiffeners and longitudinal stringers. However, in many applications the repetitive assembly and subsequent re-computation (matrix inversion) of the fully-populated and frequency-dependent BE submatrices dominate the overall computational burden of numerical simulations of the underlying vibro-acoustic problem. With respect to this limitation, the fast multipole method [33] has been developed to address the drawbacks of BEM via the acceleration of matrix–vector multiplication [8,9,34–36]. Accordingly, an iterative solver (e.g. the generalized minimal residual method: GMRES [37]) is required, which leads to the CPU time unpredictable even using some forms of preconditioners (e.g. a block diagonal preconditioner) to speed up its convergence.

Furthermore, iterative solvers are not as useful for solving linear system of equations with multiple right-hand sides [38]. Hierarchical matrices (or $\mathcal{H}$-matrices) have also been applied for fast BE calculation as conducted in [13], whereas the compressibility of the fluid is neglected. The use of traditional model reduction methods, e.g. the Padé approximation technique [39] for BE acoustic analyses is tenuous [40] even with the general proper orthogonal decomposition (POD) method which can be applied to linear as well as nonlinear systems. This is because a new small-size reduced-order counterpart has to be repeatedly updated for each frequency point of interest and obviously, it is less attractive or possibly inefficient when the frequency band of interest is wide and/or a relatively fine frequency increment is required. Therefore, it is necessary to decompose the frequency from the frequency-dependent BE matrices before the start of model reduction process. Besides, those aforementioned error indicators and adaptive techniques suffer from multiple projections of the FOM onto different low-dimensional subspaces and solution of different reduced models until a user-specified tolerance is met. The frequent comparisons for checking each other's accuracy may not be a major issue for sparse FE matrices, but can pose considerable inconvenience for BE systems in terms of the computational efficiency and memory consumption. To this effect, an adaptive Taylor-based second-order Arnoldi (AT-SOAR) approach has been proposed to generate a low-dimensional surrogate model to approximate well the original large-scale BE model [41], in which the frequency is decoupled via the series expansions and a global frequency-independent orthonormal basis is then constructed via the SOAR method to span a projection subspace.

Efficient algorithms that directly work on the complete full-order resultant matrix rather than its submatrices of a coupled system have also been introduced. One of the most generally applicable methods in the structural acoustics community is based on the solution of original high-fidelity models for snapshots (or master frequencies) at some sampling points within a frequency interval. This type of reduced basis methods can be somewhat viewed as an extension and improvement of the POD method. Apparently, the choice of certain response data is key to the quality of approximation and thus some sampling schemes are suggested, including but not limited to the Chebyshev points in a straightforward way [18] and the greedy algorithm in an iterative fashion [42].

In this work, a three-step model order reduction technique is proposed for efficient multi-frequency analyses of mutually coupled structural–acoustic systems, with the aim of providing a promising alternative to the other acceleration approaches. The matrix properties and structures of the two subsystems are fully exploited in the newly developed projection-based technique which falls into the category of moment-matching methods and renders an offline-online solution framework. The performance of the proposed method from the perspective of computational time and accuracy is evaluated using a simple elastic spherical shell and a more complex engineering structure, where both are surrounded by the infinite domain of water.

The remainder of the paper is organized as follows. In Section 2, the coupled FE–BE formulation for fluid–structure interaction problems is recalled. In Section 3, we show a three-step structure-preserving dimension reduction procedure based on the SOAR and FOAR algorithms to separately construct two groups of orthonormal bases for reduced-order modeling of both structural and acoustic subsystems, where some remarks on the practical implementation of the proposed approach as a powerful tool for multi-query vibro-acoustic analyses are outlined. Numerical verification cases and detailed discussions are highlighted in Section 4. Conclusions and future work are presented in Section 5.

2. Coupled FE-BE formulation for vibro-acoustics

2.1. Problem description

Throughout this paper, attention is focused on accelerating the solution of external structural–acoustic interaction systems modeled via the coupled FE–BE methodology for the sake of clarity since an interior problem can be easily handled through the pure FE modeling technique equipped with well-developed MOR methods, for example, see [26,30].

A typical vibro-acoustic exterior problem consists of an elastic thin-walled structure submerged into a homogeneous heavy fluid of infinite extent, as illustrated in Fig. 1. The whole problem domain can be divided into two non-overlapping fields constituted of different physical constituents, i.e. the structural domain Ω_s and the acoustic domain Ω_a and between them, Γ_{sa} indicates the coupling interface (i.e. the so-called wetted surface). From here onwards, the subscript s designates a structural quantity and similarly the subscript a denotes an acoustic component. $\mathbf{n}_s$ and $\mathbf{n}_a$ are respectively the (positive) outward normal directions to the surfaces of the corresponding domains

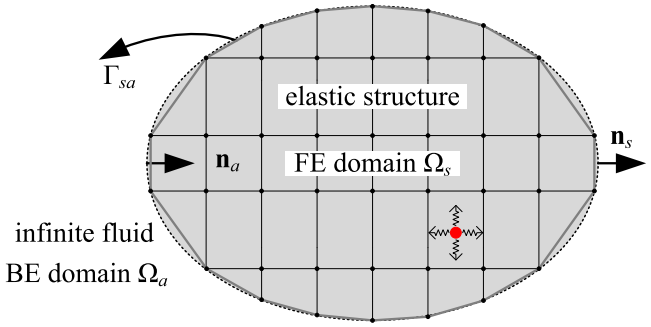

Fig. 1. General physical description for an exterior problem and its discretization.

and for the same point on the Γ_{sa}, we have $\mathbf{n}_s = -\mathbf{n}_a$. The sign convention is important for distinguishing exterior and interior problems, especially for a hollow structure. The steady-state dynamic displacements in the structure and sound pressures in the fluid medium (often referred to as the ($\mathbf{u}$, p)-formulation) result from loading terms such as a time-harmonic mechanical driving point force, denoted by a red dot in Fig. 1. Obviously, it is a strongly coupled problem, in which the acoustic environment and the elastic structure mutually interact.

2.2. Construction of the system of equations

In this work, the finite element method is used to model the dynamical field variables of the elastic structure because of its flexibility to tackle problems of high geometrical complexity and any type of (multi-) physics. The pressure field in the unbounded acoustic fluid domain is approximated using the popular boundary element method, allowing to decrease the dimension of involved problem from 3D to 2D and to satisfy the far-field boundary condition exactly. This section briefly describes the mathematical formulation and theoretical basis of these two deterministic modeling methodologies along with their coupling. For more details on this aspect, the reader can consult Refs. [4–6,8], among others. In addition, the harmonic time factor is taken as $\mathrm{e}^{-\mathrm{j}\omega t}$ and it is omitted for all time-dependent functions, where j is the imaginary unit, ω denotes the circular frequency in rad/s and t means the time variable.

The governing differential equation of a dynamic problem describing a vibrating elastic continuum is spatially discretized via the FEM which leads to the following linear system of equations

$$[\mathbf{K} - \mathrm{j}\omega\mathbf{D} - \omega^2\mathbf{M}]\mathbf{u} = \mathbf{f}_s + \mathbf{f}_a, \tag{1}$$

where $\mathbf{K}$, $\mathbf{D}$ and $\mathbf{M}$ are the stiffness, damping and mass matrices. Note that the damping included in this work is modeled as Rayleigh damping, in which case it is determined by a mass-proportional term and a stiffness-proportional term of the corresponding system, i.e. $\mathbf{D} = \alpha\mathbf{M} + \beta\mathbf{K}$, where α and β are two (known) scalar coefficients. Accordingly, all of these three matrices in Eq. (1) originated from the FE discretization are real, constant (frequency-independent) matrices ($\in \mathbb{R}^{N\times N}$) with N being the number of DOFs of structural FE model. For many practical applications, N can be very large. $\mathbf{u}$ and $\mathbf{f}_s \in \mathbb{C}^N$ are respectively the vectors of unknown nodal displacements and external mechanical nodal forces. $\mathbf{f}_a \in \mathbb{C}^N$ can be regarded as the fluid loading which is induced by the sound pressure across the common interface Γ_{sa}.

With respect to the unbounded acoustic medium, the BEM as an efficient tool is used which results in the following matrix form

$$\mathbf{H}(\omega)\mathbf{p} = \mathrm{j}\omega\rho_a\mathbf{G}(\omega)\mathbf{v}_a, \tag{2}$$

where ρ_a is the ambient fluid density; $\mathbf{p}$ and $\mathbf{v}_a \in \mathbb{C}^M$ are the vectors of the nodal values of sound pressure and normal velocity, with M being the number of DOFs of acoustic BE model; $\mathbf{G}(\omega)$ and $\mathbf{H}(\omega)$ ($\in \mathbb{C}^{M\times M}$) are respectively obtained by integrating the free-space Green's function (or called the fundamental solution) $G(\mathbf{x}, \mathbf{y})$ and its normal derivative $H(\mathbf{x}, \mathbf{y})$ over the boundary surface $\Gamma_a = \partial\Omega_a$. The two kernel functions for 3D acoustic

wave problems can be expressed as [33,43]

$$G(\mathbf{x},\mathbf{y})=\frac{\mathrm{e}^{\mathrm{j}kr}}{4\pi r},\qquad H(\mathbf{x},\mathbf{y})=\frac{\partial G(\mathbf{x},\mathbf{y})}{\partial n(\mathbf{y})}=\frac{\mathrm{e}^{\mathrm{j}kr}}{4\pi r^2}(\mathrm{j}kr-1)\frac{\partial r}{\partial n(\mathbf{y})}, \tag{3}$$

where $k=\omega/c$ is the wavenumber with c being the speed of sound; r is the distance between the source point $\mathbf{x}\in\mathbb{R}^3$ and field point $\mathbf{y}\in\mathbb{R}^3$, i.e. $r=|\mathbf{x}-\mathbf{y}|$; $n(\mathbf{y})$ is the normal direction of the boundary. Obviously, $\mathbf{G}(\omega)$ and $\mathbf{H}(\omega)$ are complex matrices whose entries depend on the frequency.

Along the interface Γ_{sa} between the structural domain Ω_s and the acoustic domain Ω_a, the following continuity constraints have to be enforced

$$\begin{cases}\mathbf{f}_a=\mathbf{C}_{sa}\mathbf{p},\\ \mathbf{v}_a=-\mathrm{j}\omega\mathbf{C}_{as}\mathbf{u},\end{cases} \tag{4}$$

where $\mathbf{C}_{sa}\in\mathbb{C}^{N\times M}$ and $\mathbf{C}_{as}\in\mathbb{C}^{M\times N}$ are the structural–acoustic coupling matrices and their sparsity patterns are determined by the percentage of the dynamical structure that is in contact with the acoustic fluid; the relationship between them is given, i.e. $\mathbf{C}_{as}=\boldsymbol{\Theta}^{-1}\mathbf{C}_{sa}^{\mathrm{T}}$ with the transpose operation $\bullet^{\mathrm{T}}$ for a matrix with real entries; $\boldsymbol{\Theta}$ is the boundary mass matrix which can be obtained by integrating the BEM (simple polynomial or spline-based) basis functions [10,44]. A fast and memory-efficient vectorized algorithm [45] is used to optimize the assembly of these sparse matrices in MATLAB.

Substituting Eq. (4) into Eqs. (1) and (2), the fully coupled FE–BE formulation for vibro-acoustic problems can be written in terms of the unknown nodal structural displacement $\mathbf{u}$ and nodal sound pressure $\mathbf{p}$ as

$$\begin{bmatrix}\mathbf{K}-\mathrm{j}\omega\mathbf{D}-\omega^2\mathbf{M} & -\mathbf{C}_{sa}\\ -\omega^2\rho_a\mathbf{G}\mathbf{C}_{as} & \mathbf{H}\end{bmatrix}\begin{bmatrix}\mathbf{u}\\ \mathbf{p}\end{bmatrix}=\begin{bmatrix}\mathbf{f}_s\\ \mathbf{0}\end{bmatrix}. \tag{5}$$

In practice, the frequency spectra of excitation generally have a broad frequency band and thus multi-frequency analysis is desired. Furthermore, a conservatively small frequency step is usually set so as not to miss any important system characteristics, e.g. (anti-) resonant peaks. In this case, Eq. (5) has to be repeatedly set up because of the frequency-dependent property of BE matrices ($\mathbf{H}(\omega)$ and $\mathbf{G}(\omega)$) and then be solved repeatedly to obtain the steady-state harmonic responses. Such a procedure, however, quickly becomes unfeasible as the size of involved model increases. Additionally, different orders of magnitude caused by the non-homogeneous nature of $\mathbf{u}$ and $\mathbf{p}$ with SI units incur Eq. (5) to be badly conditioned, which makes solution cannot be predicted well and some sophisticated scaling (e.g. using the Young's modulus of structures as a scaling factor [18]) and/or preconditioning (e.g. block diagonal preconditioner [9]) techniques are often required. Therefore, there is a pressing need for powerful computational approaches, capable of solving Eq. (5) at low cost and with high precision.

Typically, the FE system matrices are symmetric, sparsely populated and have a banded structure; while the BE system matrices are non-symmetric, fully populated but in general, their dimension is (relatively) smaller than that of FE matrices, i.e. $M<N$. The coupling matrices are sparse rectangular matrices due to the fact that only nodal DOFs located on the interface Γ_{sa} with contributions in the normal direction yield nonzero values. In the next section, in order to improve the computational efficiency of frequency sweep analyses for a general hybrid FE–BE numerical model, a three-step model order reduction solution scheme is proposed, where the matrix properties and specific forms of each subsystem in Eq. (5) are utilized.

3. Three-step MOR strategy

The entire workflow for performing efficient frequency-domain simulations of vibro-acoustic FE–BE models using the proposed automatic MOR solution procedure is schematically summarized in Fig. 2. In what follows, the general idea behind this method and its detailed branches are explained step by step.

3.1. MOR for structural FE subsystem

In the first step, the sparsity, banded-structure and frequency-independence of the FE dynamic matrix triplet ($\mathbf{K}$, $\mathbf{D}$, $\mathbf{M}$) can be used without loss of generality. To enable fast vibro-acoustic evaluations, the well-known second-order Arnoldi (SOAR) procedure for constructing an orthonormal basis of the second-order Krylov subspace $\mathcal{G}_{n_\star}(\mathbf{A},\mathbf{B};\mathbf{r}_0)$

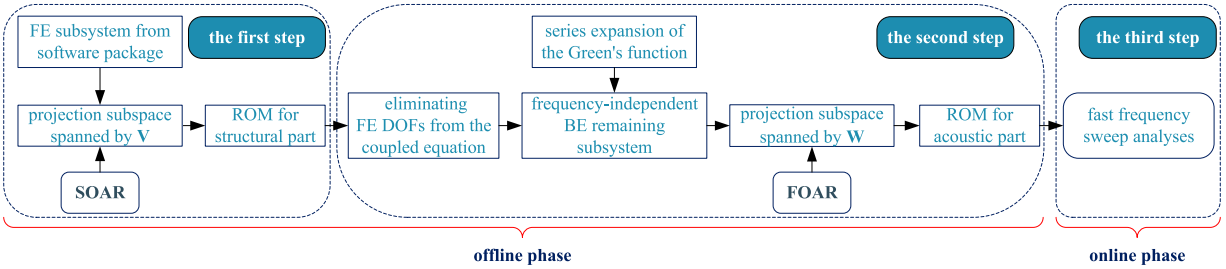

Fig. 2. Flowchart of the proposed method.

is applied to reduce the number of elastic DOFs (and the associated computational cost and storage). The second-order Krylov sequence $\{\mathbf{r}_\ell\}$ which is orthogonalized by means of a modified Gram–Schmidt process is generated by a recurrence relation as

$$\begin{cases} \mathbf{r}_1 = \mathbf{A}\mathbf{r}_0, \\ \mathbf{r}_\ell = \mathbf{A}\mathbf{r}_{\ell-1} + \mathbf{B}\mathbf{r}_{\ell-2}, \quad \text{for } 2 \le \ell \le n_\star - 1 \end{cases} \tag{6}$$

where $\mathbf{A} = -\tilde{\mathbf{K}}^{-1}\tilde{\mathbf{D}}$ and $\mathbf{B} = -\tilde{\mathbf{K}}^{-1}\mathbf{M}$. The transformed matrices $\tilde{\mathbf{K}}$ and $\tilde{\mathbf{D}}$ around a prescribed expansion point $s_\star$ are given by

$$\tilde{\mathbf{K}} = \mathbf{K} + s_\star\mathbf{D} + s_\star^2\mathbf{M}, \qquad \tilde{\mathbf{D}} = \mathbf{D} + 2s_\star\mathbf{M}. \tag{7}$$

The inverse of $\tilde{\mathbf{K}}$ is computed in an inexpensive way by using its factorized form, such as an LU decomposition. Clearly, the factorization has to be carried out only once and then can be re-used at every subsequent iteration step for the construction of a local orthonormal basis $\mathbf{R}_\star$, where $\text{span}\{\mathbf{R}_\star\} = \mathcal{G}_{n_\star}(\mathbf{A}, \mathbf{B}; \mathbf{r}_0) = \text{span}\{\mathbf{r}_0, \mathbf{r}_1, \mathbf{r}_2, \ldots, \mathbf{r}_{n_\star-1}\}$. In order to comply with the mathematical and actual physical meanings (i.e. the complex variable $s = \mathrm{j}\omega$), the selection of purely imaginary number for $s_\star$ is suggested. The nonzero starting vector $\mathbf{r}_0$ is important as the remaining column vectors of $\{\mathbf{r}_\ell\}$ are partially determined by it according to Eq. (6). In this work, it is simply given as the response (static deflection) of the elastic structure about $s_\star$ under the mechanical loading $\mathbf{f}_s$ since the acoustic loading $\mathbf{f}_a$ is unknown, i.e. $\mathbf{r}_0 = \tilde{\mathbf{K}}^{-1}\mathbf{f}_s$.

On the one hand, a single-point expansion is often not enough to capture dynamical features of the FOM over a broad frequency range. On the other hand, the offline construction of a global orthonormal matrix cannot be prohibitively expensive. Therefore, a very limited $\star$ (in this work $\star = 1, 2, 3$) number of expansion points is expected, which implies that only three linear systems with the full size N need to be solved. This way three local orthonormal bases $\mathbf{R}_1, \mathbf{R}_2, \mathbf{R}_3$ with different dimensions $n_\star$ are achieved. Afterwards, these bases are combined by column stacking and re-orthogonalized by an economy-size of the Singular Value Decomposition (SVD), namely,

$$\mathbf{V}\boldsymbol{\Sigma}\mathbf{U}^{\mathrm{H}} = \text{svd}([\mathbf{R}_1, \mathbf{R}_2, \mathbf{R}_3]), \tag{8}$$

where $\mathbf{V}$ and $\mathbf{U}$ are complex unitary matrices whose columns are called the left- and right-singular vectors, respectively; the superscript $\bullet^{\mathrm{H}}$ designates the Hermitian transpose; $\boldsymbol{\Sigma}$ is a rectangular diagonal matrix whose elements σ are known as the singular values. In general, these are non-negative real numbers which decrease quite fast. Therefore, the truncation of the left singular vectors is commonly used to filter out components with very small singular values so as to reduce the dimension of the global orthonormal basis while still carrying the most essential information of the system, by setting a threshold to the ratio of those singular values with respect to the first one (i.e. the largest one σ_1). Unless otherwise stated, the threshold value 10^{-10} will be chosen in the following, which satisfies

$$\begin{aligned} &\frac{\sigma_\kappa}{\sigma_1} \ge 10^{-10}, \qquad \kappa = 1, \ldots, n \\ &\Rightarrow \mathbf{V} = \mathbf{V}(:, 1:n), \end{aligned} \tag{9}$$

where n ($\le n_1 + n_2 + n_3$) denotes the final dimension of the columns of the global orthonormal basis $\mathbf{V} \in \mathbb{C}^{N\times n}$. To derive a ROM, the full-order state $\mathbf{u} \in \mathbb{C}^N$ is approximated by the reduced state vector $\mathbf{u}_n \in \mathbb{C}^n$ in the subspace

$\mathcal{G}_n$ spanned by the linearly independent column basis vectors of $\mathbf{V}$

$$\mathbf{u} \approx \mathbf{V}\mathbf{u}_n. \tag{10}$$

In most cases, it holds that $n \ll N$. Through application of the one-sided Galerkin projection, a reduced-order model which preserves the structure and crucial dynamics of the original full system reads

$$[\mathbf{K}_n - \mathrm{j}\omega\mathbf{D}_n - \omega^2\mathbf{M}_n]\mathbf{u}_n = \mathbf{f}_{s,n} + \mathbf{f}_{a,n} = \mathbf{f}_{s,n} + \mathbf{C}_{sa,n}\mathbf{p}, \tag{11}$$

where $\mathbf{K}_n = \mathbf{V}^{\mathrm{H}}\mathbf{K}\mathbf{V}$, $\mathbf{D}_n = \mathbf{V}^{\mathrm{H}}\mathbf{D}\mathbf{V}$, $\mathbf{M}_n = \mathbf{V}^{\mathrm{H}}\mathbf{M}\mathbf{V}$, $\mathbf{f}_{s,n} = \mathbf{V}^{\mathrm{H}}\mathbf{f}_s$ and $\mathbf{C}_{sa,n} = \mathbf{V}^{\mathrm{H}}\mathbf{C}_{sa}$. Thereafter, the solution of the original second-order dynamical system can be represented well by solving the compact ROM, which is typically several orders of magnitude smaller in size and consequently much easier/faster to compute as compared to the FOM.

In addition, viscoelastic or porous materials are often used in many industrial sectors and their nonlinear mathematical descriptions can be inserted into conventional FE equations with constant properties by replacing the frequency-independent system matrices with frequency-dependent ones, which harms the solving efficiency and puts more computational difficulties. However, with a transformation technique based on algebraic polynomials to deal with the frequency-dependent terms, which was proposed by Xie et al. [31,46], the presented SOAR algorithm can be applied for reduced order modeling of dynamical systems with (mono- or multi-layered) add-on viscoelastic or porous damping treatments as well.

3.2. MOR for acoustic BE subsystem

After substituting the resulting ROM expression Eq. (11) into Eq. (5) and eliminating the structural DOFs, it can be easily derived that

$$\mathbf{H}\mathbf{p} - \mathbf{G}\mathbf{E}\mathbf{C}_{sa,n}\mathbf{p} = \mathbf{G}\mathbf{E}\mathbf{f}_{s,n}, \tag{12}$$

where $\mathbf{E} = \omega^2\rho_a\mathbf{C}_{as,n}\mathbf{Z}_n^{-1}$ with the coupling matrix $\mathbf{C}_{as,n} = \mathbf{C}_{as}\mathbf{V}$ and the reduced dynamical stiffness matrix $\mathbf{Z}_n = \mathbf{K}_n - \mathrm{j}\omega\mathbf{D}_n - \omega^2\mathbf{M}_n$.

For the purpose of model reduction the system matrices and projection operators are expected to be independent of the frequency. Therefore, before we proceed to the construction of an orthonormal basis for the BE subsystem, the wavenumber is factored out from the exponential function in Eq. (3) by the use of Taylor's theorem about a fixed point k_* with the first $L+1$ terms

$$\mathrm{e}^{\mathrm{j}kr} = \mathrm{e}^{\mathrm{j}k_*r}\sum_{l=0}^{L}\frac{(\mathrm{j}r)^l(k-k_*)^l}{l!}. \tag{13}$$

It is clear that the effectiveness of this affine decomposition over a broad frequency range depends on the suitable number of expansion representations, which can be empirically determined by a cheap error estimator based on the Lagrange remainder [41]. After that, substituting Eq. (13) into Eq. (12) and according to the order of wavenumber k, Eq. (12) can be rewritten in an equivalent form as

$$\left[\sum_{l=0}^{L}\frac{(k-k_*)^l}{l!}(k\bar{\mathbf{H}}_{l+1} - \bar{\mathbf{H}}_l - \bar{\mathbf{G}}_l\mathbf{E}\mathbf{C}_{sa,n})\right]\mathbf{p} = \sum_{l=0}^{L}\frac{(k-k_*)^l}{l!}\bar{\mathbf{G}}_l\mathbf{E}\mathbf{f}_{s,n}, \tag{14}$$

where

$$\bar{\mathbf{H}}_l = \int_{\Gamma_a}(\mathrm{j}r)^l\frac{\mathrm{e}^{\mathrm{j}k_*r}}{4\pi r^2}\frac{\partial r}{\partial n(\mathbf{y})}\mathrm{d}\Gamma, \qquad \bar{\mathbf{G}}_l = \int_{\Gamma_a}(\mathrm{j}r)^l\frac{\mathrm{e}^{\mathrm{j}k_*r}}{4\pi r}\mathrm{d}\Gamma. \tag{15}$$

In this manner, the dense frequency-dependent BE system matrices $\mathbf{G}$ and $\mathbf{H}$ ($\in \mathbb{C}^{M\times M}$) are decoupled as a finite sum of frequency-dependent scalar functions multiplied by frequency-independent system matrices $\bar{\mathbf{G}}_l$ and $\bar{\mathbf{H}}_l$ ($\in \mathbb{C}^{M\times M}$), where their integral calculations need to be performed only once instead of at each frequency of interest, thereby yielding a rather efficient matrix assembly procedure. In order to further reduce the computational cost of multi-frequency solution of the acoustic BE subsystem, the well-established MOR technique based on the standard linear Krylov subspace which is spanned by a sequence of $m_\star$ column vectors, i.e. $\mathcal{K}_{m_\star}(\mathbf{Q},\mathbf{g}) =$

span{$\mathbf{g}, \mathbf{Qg}, \mathbf{Q}^2\mathbf{g}, \ldots, \mathbf{Q}^{m_\star-1}\mathbf{g}$} is applied. To this end, only the system matrices corresponding to the selected expansion point $k_\star$ in the series expanded Eq. (14) (i.e. when $l = 0$) are used to generate this projection subspace. To be more specific, we have the following

$$[k\bar{\mathbf{H}}_1 - \bar{\mathbf{H}}_0 - \bar{\mathbf{G}}_0\mathbf{E}_0\mathbf{C}_{sa,n}]\mathbf{p} = \bar{\mathbf{G}}_0\mathbf{E}_0\mathbf{f}_{s,n}, \tag{16}$$

where $\mathbf{E}_0 \in \mathbb{C}^{M\times n}$ is obtained from $\mathbf{E}$ by setting $\omega = k_\star c$. One would wonder why the system matrices around the expansion point $k_\star$ can be used to construct an orthonormal basis with sufficient accuracy for projection. The reason is that entries in different $\bar{\mathbf{H}}_l$ or $\bar{\mathbf{G}}_l$ differ by only one coefficient jr (see Eq. (15)). Therefore, the system matrices $\bar{\mathbf{H}}_1$, $\bar{\mathbf{H}}_0$ and $\bar{\mathbf{G}}_0$ without more derivative matrices in fact maintain inherent information about the original system of equations.

In order to conform and further unite the model reduction process for the structural FE part, the relationship between the two expansion points $s_\star$ and $k_\star$ is matched, i.e. $s_\star = \mathrm{j}k_\star c$. In addition, notice the difference between k_* and $k_\star$, where k_* is a single point used to approximate the kernels by the Taylor series over the considered frequency range (see Eq. (13)), while $k_\star$ represents (usually more than one) selected expansion points used to construct a global projection matrix.

Thereafter, with the help of the first-order Arnoldi (FOAR) process, a local frequency-independent orthonormal basis can be iteratively generated with a square matrix $\mathbf{Q}$ and a starting vector $\mathbf{g}$, which are defined as

$$\begin{cases}\mathbf{Q} = -(k_\star\bar{\mathbf{H}}_1 - \bar{\mathbf{H}}_0 - \bar{\mathbf{G}}_0\mathbf{E}_0\mathbf{C}_{sa,n})^{-1}\bar{\mathbf{H}}_1, \\ \mathbf{g} = +(k_\star\bar{\mathbf{H}}_1 - \bar{\mathbf{H}}_0 - \bar{\mathbf{G}}_0\mathbf{E}_0\mathbf{C}_{sa,n})^{-1}\bar{\mathbf{G}}_0\mathbf{E}_0\mathbf{f}_{s,n}.\end{cases} \tag{17}$$

Note that $\mathbf{Q}$ and $\mathbf{g}$ have identical inverted matrices, which allows them to be solved at the same time, requiring only a single LU decomposition for one $k_\star$. The local behavior of polynomial approximation based on the Taylor series implies that dynamical characteristics far away from the chosen expansion point $k_\star$ are difficult to capture and thus their multiples are often allocated. As before, three expansion points are selected along the frequency axis. Because each one has its own local orthonormal bases, an orthogonalization procedure based on the thin SVD should be executed to compress them into a union of reduction bases $\mathbf{W} \in \mathbb{C}^{M\times m}$ (m: the number of DOFs of the generated BE ROM) for computational efficiency. Then the BE original DOFs $\mathbf{p}$ can be favorably approximated by another vector $\mathbf{p}_m$ constrained to stay in the Krylov subspace $\mathcal{K}_m$ spanned by the columns of $\mathbf{W}$, namely,

$$\mathbf{p} \approx \mathbf{W}\mathbf{p}_m, \tag{18}$$

with $\mathbf{p}_m \in \mathbb{C}^m$ and normally $m \ll M$. Substituting Eq. (18) into Eq. (14) and left-multiplying the associated equation by the conjugate transpose of the matrix $\mathbf{W}$, a reduced-order model with order m can be naturally obtained. However, this is not really a memory-efficient projection process as multiple dense system matrices $\bar{\mathbf{H}}_l$ and $\bar{\mathbf{G}}_l$ ($\in \mathbb{C}^{M\times M}$) need to be explicitly formed. The required storage for these matrices scales with $\mathcal{O}((2L+3)M^2)$, which may quickly exceed the available memory. Therefore, a fast and memory saving column-by-column projection is developed in such a way that the memory limitation of polynomial approximation approaches by using various forms of expansions of the integral kernels [19,47,48] for a given computer can be accommodated. In other words, once one column in the BE frequency-decoupled matrices of Eq. (15) is assembled for one field point and all the source points, a left-sided projection is immediately implemented until all the field points are looped. In this way, the storage requirement is reduced from $\mathcal{O}((2L+3)M^2)$ to $\mathcal{O}((2L+3)mM)$, followed by a right-sided projection for the resulting matrices, the memory usage is further decreased to $\mathcal{O}((2L+3)m^2)$, as detailed in [41]. As a result, Eq. (14) becomes of the form

$$\left[\sum_{l=0}^{L}\frac{(k-k_*)^l}{l!}(k\bar{\mathbf{H}}_{l+1,m} - \bar{\mathbf{H}}_{l,m} - \bar{\mathbf{G}}_{l,m}\mathbf{E}\mathbf{C}_{sa,nm})\right]\mathbf{p}_m = \sum_{l=0}^{L}\frac{(k-k_*)^l}{l!}\bar{\mathbf{G}}_{l,m}\mathbf{E}\mathbf{f}_{s,n}, \tag{19}$$

where $\bar{\mathbf{H}}_{l,m} = \mathbf{W}^{\mathrm{H}}\bar{\mathbf{H}}_l\mathbf{W}$, $\bar{\mathbf{G}}_{l,m} = \mathbf{W}^{\mathrm{H}}\bar{\mathbf{G}}_l$ and $\mathbf{C}_{sa,nm} = \mathbf{C}_{sa,n}\mathbf{W}$.

So far, the offline phase for constructing of two low-dimensional subspaces for both the structural and fluid partitions and further projecting the frequency-independent submatrices of the original model onto these subspaces has been accomplished. Three remarks are provided for the extension of the presented strategy.

Remark 1. It has been known that the classical linear Krylov subspace-based first-order Arnoldi method is a special case of the second-order Krylov subspace-based second-order Arnoldi algorithm without the second-order term.

Therefore, one of the main advantages of the proposed solution concept is that it is very general and can be easily applied to other fluid–structure coupling formulations. For example, if no (Rayleigh/viscoelastic/porous) damping is included for FE elastic structures, then the fast FOAR technique as mentioned above for BE acoustic fields instead of the SOAR algorithm is deployed to accelerate structural vibration analyses by considering the square of frequency as a single variable. In addition, if the Burton–Miller formulation [49] is adopted to overcome the fictitious eigenfrequency difficulty existing in the conventional boundary integral equation (CBIE) for exterior acoustic wave problems, then the efficient SOAR algorithm can be implemented to economize numerical simulations of both the FE subsystem and the BE subsystem. This is because that by reformulating the CBIE and its normal derivative equation at given expansion point, a second-order dynamical system rather than its first-order equivalent is achieved [41]. All these situations can be handled without any restriction, revealing the beneficial versatility and generality of the newly presented approach for the study of strongly coupled external vibro-acoustics modeled via the hybrid FE–BE method. Although investigations in this work are limited to exterior problems on account of underwater maritime applications, the proposed technique can be directly used for an interior problem, where the formulation is established for a finite volume of an acoustic medium (fully or partially) closed by a vibrating structure with particular boundary conditions.

Remark 2. For practical implementation of the proposed model reduction technique, it is important to determine the proper number of expansion points and their associated orders such that a ROM with satisfactory accuracy can be obtained. In that sense there is a common trade-off between ROM size and computational cost in the offline phase. The most commonly used automatic algorithms in literature often involve different trial-error tests and/or suffer from the necessity of solving reference models for validation until a prescribed threshold is satisfied, which are undesirable in many practical applications. Therefore, a cheap adaptive strategy without recourse to the FOM and comparison of different ROMs is favored for large-scale vibro-acoustic problems. It should be noted that all moment-matching approaches are locally effective in nature [21] and will stagnate in accuracy when a certain value of order is reached, which means that in slowing convergence range more matched moments do not lead to a more accurate representation of the original dynamical system. Motivated by this fact, three expansion points are discretely deployed herein in order to ensure the global approximation quality of reduced systems in large frequency domains. Afterwards, the success of an automated reduction process merely relies on the dimension of orthonormal vectors to be calculated for each expansion point. For the FE submodels, the condition number of an upper Hessenberg matrix in SOAR together with a pre-specified upper bound `lub` as the stopping criterion can be leveraged to decide the amount of iterations required for convergence [41,50]. As for the BE submodels, $\hat{L}$ terms of the Taylor series near each expansion point $k_\star$ can be assigned according to the Lagrange remainder and then the related order is empirically given as $4\hat{L}$ (i.e. $m_\star = 4\hat{L}$) within its desired radius of accuracy. Note the difference between L and $\hat{L}$ (it holds that $L \geq \hat{L}$), where L is the highest order of the Taylor series used to approximate the kernels over the whole frequency range of interest (see Eq. (13)), while $\hat{L}$ is the one with respect to three subsets of the considered frequency range (each expansion point $k_\star$ has its own effective frequency interval), as already investigated in more detail in previous work [41]. Therefore, both the model reduction process and the subsequent analyses that are performed using the ROM are computationally efficient, even taking into account really large systems.

Remark 3. If the considered frequency range is too wide or the elastic structure is large-sized, the broadband frequency range of interest can be divided into several frequency subintervals. Within each interval, the proposed MOR process can be used to accelerate the numerical simulation and to the end its multi-point counterparts covering the entire frequency band are formed. In this way, the maximum expansion term L in Eq. (13) can also be reduced, which is favored for the approximation of the kernel functions using Taylor polynomials. This is because double-precision numbers are only accurate up to 15 digits, the numerical error (e.g. incurred in the factorial operation for a large integer L) can be alleviated.

Next, the quick assembly of the whole ROM and solution at multiple frequencies for broadband vibro-acoustic simulations will be elaborated.

3.3. Online multi-frequency analysis

In the online phase, we need to compute the frequency-dependent coefficients in Eq. (14) for each frequency and then a robust ROM can be rapidly created from the offline stored reduced matrices/vectors by the use of

straightforward multiplication and summation operations. Combining Eqs. (11) and (19) yields

$$\begin{bmatrix} \mathbf{K}_n - \mathrm{j}\omega\mathbf{D}_n - \omega^2\mathbf{M}_n & -\mathbf{C}_{sa,nm} \\ -\omega^2\rho_a\mathbf{G}_m\mathbf{C}_{as,n} & \mathbf{H}_m \end{bmatrix} \begin{bmatrix} \mathbf{u}_n \\ \mathbf{p}_m \end{bmatrix} = \begin{bmatrix} \mathbf{f}_{s,n} \\ \mathbf{0} \end{bmatrix}, \tag{20}$$

where

$$\mathbf{G}_m = \sum_{l=0}^{L} \frac{(k-k_*)^l}{l!}\bar{\mathbf{G}}_{l,m}, \qquad \mathbf{H}_m = \sum_{l=0}^{L} \frac{(k-k_*)^l}{l!}(k\bar{\mathbf{H}}_{l+1,m} - \bar{\mathbf{H}}_{l,m}). \tag{21}$$

It is clear that the structure of the original global system represented in Eq. (5) with its four physically distinct submatrices is preserved. As such, the proposed three-step MOR strategy is a structure-preserving dimension reduction algorithm for vibro-acoustic multi-frequency problems simulated through the coupled FE–BE technique. Note that inside the considered frequency range, the ROM is an accurate approximation of the FOM, but beyond that it is not guaranteed to be valid any more. It is possible to extend the width of effective frequency band but this will increase the number of DOFs in the ROM (i.e. the ROM size).

The CPU time and storage required for the online frequency sweep analyses only depend on the number of the series representations and the dimension of the generated ROM, thereby reducing the computational complexity dramatically compared to the brute direct evaluation of the high-dimensional original model. As a by-product, the projection step via the congruence transformations can potentially yield better conditioned systems since multiplying with an orthonormal basis on both sides of the dynamical equation can be viewed as preconditioning. Accordingly, due to the much lower dimension, the linear system of equation (20) can be easily solved using the built-in direct solver `mldivide` in MATLAB which selects the appropriate routine according to the properties of the coefficient matrix.

4. Numerical experiments

In this section, we present two numerical examples, both on an academic case and on a more practical application case, to demonstrate the high performance of the three-step model order reduction procedure. All our codes are implemented in MATLAB R2019a. All data regarding condensed system matrices (by means of the constraint elimination) of FE substructures, node coordinates and elements connectivity information on the surface mesh are assembled and extracted from COMSOL MULTIPHYSICS with MATLAB. An interactive interface to the commercial FE package is set up [51] and research codes are developed for FE–BE coupling terms along the fluid–structure interface and BE modeling of exterior acoustic fields, which have good flexibility to deal with real-life complex-shaped structures in great detail. Both verification tests are carried out on a Windows workstation with Intel(R) Xeon(R) Gold 6132 CPU at 2.60 GHz and 64 GB of RAM.

The six-node quadratic (shape functions) triangular shell elements for the outside surface of the FE part and constant triangular elements for the BE part are applied, which make the coupling of both methodologies can be conducted directly and further the evaluation of singular integrals can be performed analytically. In both case studies, the acoustic media of infinite volume are assumed to be water for which the mass density and speed of sound are respectively taken as $\rho_a = 1000\ \mathrm{kg/m^3}$ and $c = 1500\ \mathrm{m/s}$; the structures are made from steel with material parameters $E = 210$ GPa, $\rho_s = 7900\ \mathrm{kg/m^3}$, $\nu = 0.3$; the real scalar coefficients of Rayleigh damping are set to $\alpha = 10$ and $\beta = 10^{-7}$.

4.1. Elastic sphere submerged in an infinite fluid

The first example is a classical fluid–structure benchmark model, which comprises an elastic spherical shell with a radius of 5 m and a thickness of 0.05 m surrounded by water. This underlying coupled system without structural damping has been extensively studied and the analytical solution for the displacement at any point on the sphere or fluid pressure at any point inside the acoustic domain is available, see [3,9,10,18,42,44] and it serves as the reference for a full 3D solution. The structure is excited by a harmonic unit point force at coordinates $(0, 0, -5)$ m along the global positive z-direction on the outer-surface side, where the origin is located at its center. The sphere is discretized using 12620 triangular elements with 25242 nodes and 6312 mesh vertices (as displayed in Fig. 4(a)), which results in an FE shell submodel of order $N = 126210$ and a BE acoustic submodel of order $M = 12620$.

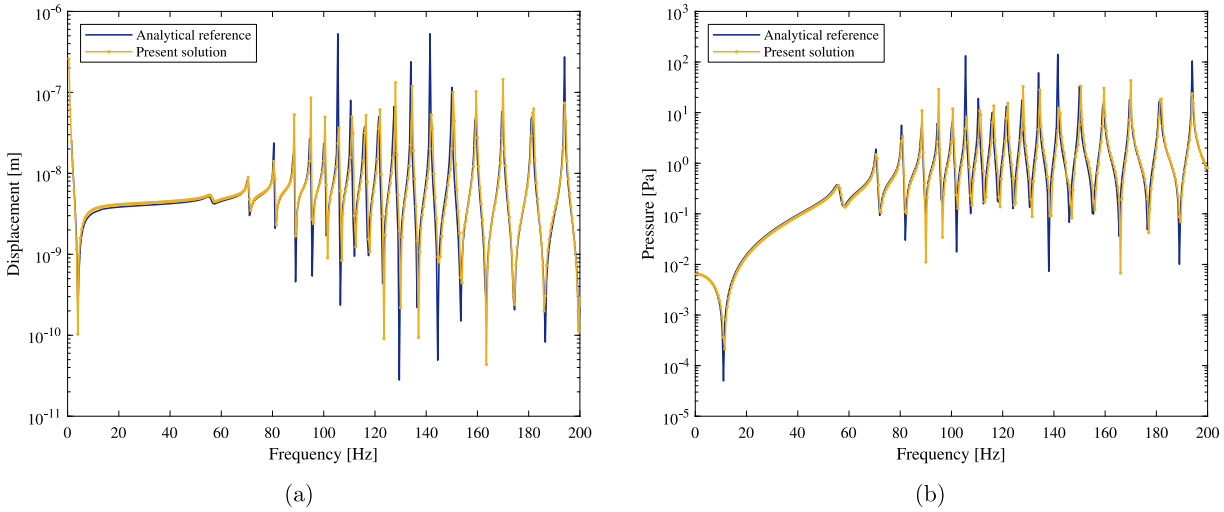

Fig. 3. Dynamical responses of a submerged steel sphere at the point $(0, 0, -5)$ m: (a) Displacement; (b) Sound pressure.

In this example, the largest distance between a field point and a source point is the diameter of sphere. According to the deduced error bound in [41], the maximum expansion term $L = 13$ around the selected base point $k_* = 2\pi \times 125/c$ is sufficient for obtaining reliable solution within the considered frequency range from $f_{\min} = 0.5$ Hz to $f_{\max} = 200$ Hz with a 0.5 Hz frequency step. In order to construct a proper projection subspace, three expansion points, i.e. $s_\star = \mathrm{j}ck_\star = 2\pi\mathrm{j} \times [75, 125, 180]$ are designated to perform the hybrid SOAR–FOAR algorithm. Expansion points are advisable to be located in the higher frequency range as there is more system (modal) information at play and thus more orthonormal vectors are subsequently required to capture the inherent dynamical characteristics of the original model over there. The default upper bound for the condition number of the upper Hessenberg matrix in the SOAR procedure is practically chosen as: $\texttt{lub} = 10^{10}$ and the associated supremum of order for the reduction basis corresponding to each $k_\star$ in FOAR is controlled and truncated by the Lagrange remainder, which leads to $4\hat{L} = 52$ for this case. In this way, the application of the proposed automatic reduction technique results in a reduced-order model with a size of only 292 DOFs, where $n = 133$ for the structural subsystem and $m = 159$ for the acoustic subsystem. Note that in SOAR- or FOAR-algorithm looping n or m times will get $n + 1$ or $m + 1$ columns of orthonormal matrix since the starting vector $\mathbf{r}_0$ or $\mathbf{g}$ is given before iteration.

4.1.1. Case without damping

The present results are first compared with the undamped analytical solutions to confirm the validity of the (numerical and exact) integration for BE matrices and also the construction of coupling terms $\mathbf{C}_{sa}$ and $\mathbf{C}_{as}$. As mentioned in Remark 1, if no damping is considered for the structural part, then the FOAR–FOAR algorithm instead of the hybrid SOAR–FOAR procedure can be used.

The parameter settings for the implementation of FOAR–FOAR algorithm are the same as aforementioned for the SOAR–FOAR, i.e. with the same expansion points $s_\star$ and the same reduced orders n and m. Fig. 3 graphically depicts the absolute values of the analytical/predicted ($+z$ direction) displacement and sound pressure at the point $(0, 0, -5)$ m where the force acts. It is clear that the constructed ROM delivers satisfactorily accurate approximation over the entire frequency band of interest, thereby allowing for a more refined frequency grids to be sampled for dynamical response analyses. This is important since in practice the fine frequency increments (even oversampled resolution) are preferred to thoroughly understand intrinsic dynamic properties and also to identify some parameters (e.g. natural frequencies, damping ratio, etc.) of vibro-acoustic systems. In fact, as the structure is considered to be undamped for the derivation of analytical/numerical solution, it is supposed to reach an infinite level at resonant frequencies, but is limited due to the frequency calculation step ($\Delta f = 0.5$ Hz in this case). In addition, eighteen response peaks can be intuitively distinguished from the character of (both the displacement and pressure) response functions at this particular node.

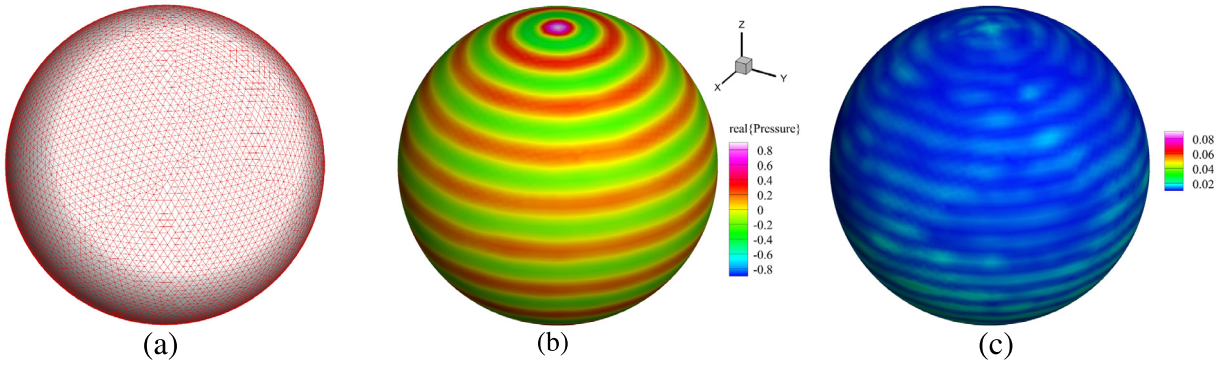

Fig. 4. (a) Problem geometry and its surface mesh; (b) Contour plot of the real component of surface acoustic pressure and (c) Its corresponding relative error with respect to the analytical solution at 200 Hz.

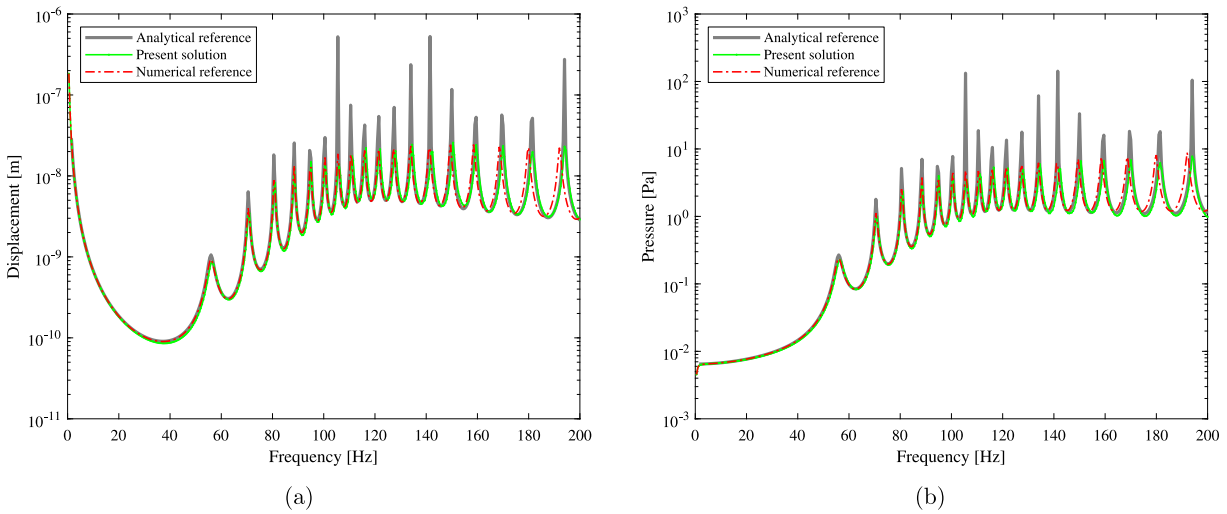

Fig. 5. Dynamical responses of a submerged steel sphere at the point $(0, 0, 5)$ m: (a) Displacement; (b) Sound pressure.

Moreover, with the adaptively generated ROM, displacement quantities at any other node on the shell surface and sound characteristics at any field point in the exterior domain (and its boundary) can be readily evaluated. As an example, Fig. 4(b) shows a contour plot of the real part of acoustic pressure distributions at $f = 200$ Hz obtained from the ROM. It is obvious that the constructed ROM accurately predicts the surface pressure at all the BE independent DOFs, as shown in Fig. 4(c), where the error with respect to the analytical solution is mostly in the order of an engineering accuracy of 1%.

4.1.2. Case with damping

To demonstrate the beneficial versatility and generality of the proposed three-step MOR methodology, the structural dynamical model incorporating Rayleigh damping (with scalar coefficients $\alpha = 10$ and $\beta = 10^{-7}$) is studied and the SOAR algorithm is applied for reduced-order modeling of the large-scale second-order system of Eq. (1). Fig. 5 shows the absolute values of the analytical/predicted ($+z$ direction) displacement and sound pressure at the point $(0, 0, 5)$ m located on the surface of the sphere (i.e. radius 5 m and azimuthal angle 180° with respect to the excitation point), from which it is clear that the present solutions match the analytical ones well. The slight difference can be attributed to the presence of Rayleigh damping and thus resonant peaks are suppressed.

In order to further investigate the performance and assess the approximation quality, the present results of the ROM with reduced order 292 are also compared to the solutions obtained from the commercial software package COMSOL, where the BEM in Acoustics Module can be seamlessly coupled to FEM-based Structural Mechanics

Table 1
Calculation time for the three substeps of the proposed MOR process.

	Step 1 /structural FE part/	Step 2 /acoustic BE part/	Step 3 /frequency sweeps/
Wall-clock time [s]	146	6228	5

Module. The same mesh discretization with quadratic elements for the spherical shell is adopted, while linear/linear Lagrange shape functions for the pressure/normal acceleration are employed to model the acoustic field. This way the resulting system of equations (similar to the form Eq. (5)) has 139224 complex-valued DOFs, which are nearly equivalent to those of the proposed MOR approach with in total 138830 DOFs, thereby allowing for a fair comparison. Very good agreement can be observed, as illustrated in Fig. 5 and even better, the current results appear to be somewhat more accurate than that calculated from the software package, especially in the higher frequency range.

In this case, with a fully vectorized algorithm [45], the assembly of those two coupling matrices $\mathbf{C}_{sa}$ and $\mathbf{C}_{as}$ ($\in \mathbb{R}^{N\times M}$ and $\mathbb{R}^{M\times N}$) is done in less than one second. Except this, the wall-clock time used for obtaining the transfer function in one instance of the FOM is more than 4.5 h, and the elapsed time required for the solution of in total 400 large-scale algebraic system of equations can be directly estimated since it grows linearly with the number of sampled frequencies. The CPU time of the presented three-step MOR approach is 1.77 h. The speed-up factor compared to the brute force approach based on the FOM evaluation is therefore better than three full orders of magnitude and the benefit from both reduced DOFs and runtime viewpoints is apparent. Specifically, the processing time for constructing the orthonormal basis $\mathbf{V}$ (the first step) and generating the projection matrix $\mathbf{W}$ (the second step) is respectively 146 s and 1.73 h, as reported in Table 1. Performing the subsequent online frequency sweep (the third step) only marginally contributes to the overall computational cost (i.e. increases by 5 s), which verifies that the cost involved in computing the response functions using the previously established ROM is almost negligible. It is obvious that the most time-consuming part of the whole MOR process is the second step, which corresponds to the dimension reduction of the BE submodel. The total CPU time needed for simulating this coupled structural–acoustic problem using the commercial dedicated FE–BE method is 13.8 h, where the GMRES solver and sparse approximate inverse (SAI) with the default preconditioner and the default settings are used, resulting in an average of 2.07 min for each frequency point. Thus, despite the fact that almost equal DOFs with the same mesh discretization are analyzed on the computer with the same configuration, the proposed SOAR–FOAR technique runs approximately 8 times faster. Note that all CPU time data are averaged over a couple of calculations.

4.2. Underwater vehicle submerged in water

The second example illustrates the ability of the proposed three-step model order reduction methodology to analyze the vibro-acoustic behavior of a hull involving complicated internal built-up structure immersed in an infinite extent filled with water, as represented in Fig. 6. The model's bounding box has dimensions 11.85 m × 2 m × 2 m, which consists of a 7 m long cylinder with a diameter of 2 m, a 2.4 m long cone with radii of 1 m and 0.4 m at its large and small edges and on both sides closed by a 2.2 m ellipsoid endcap and a 0.25 m sphere endcap. Eight circumferential rings and four longitudinal stringers with their width as 0.2 m are mounted to reinforce the shell structure. Additionally, an inner cylinder with a radius of 0.8 m and two-end baffles is attached and its length is equal to that of the outer cylinder. Assuming that all shell components, ring stiffeners and longitudinal stringers are made of steel with Rayleigh damping and have a uniform thickness of 0.04 m. The dynamical system is subjected to four unit point forces in the $+z$ direction whose positions are inside the hull at the points $(2, 0, -0.8)$ m, $(3, 0, -0.8)$ m, $(4, 0, -0.8)$ m and $(5, 0, -0.8)$ m, where the origin is located in the center of the first baffle.

The internal structure is meshed with 11352 nine-node quadratic (shape functions) quadrilateral curved shell elements and the outer hull which is in contact with the acoustic domain is discretized by 21392 six-node quadratic triangular shell elements. This way the total number of DOFs in the resulting FE–BE hybrid model is 457094, where $N = 435702$ for the FE displacement field and $M = 21392$ for the BE sound pressure field. The center of Taylor expansion is defined at a given point $k_* = 2\pi \times 350/c$ over the frequency range from $f_{\min} = 1$ Hz to $f_{\max} = 500$ Hz with increment of 1 Hz. The maximum distance of two points on the submerged structure is its

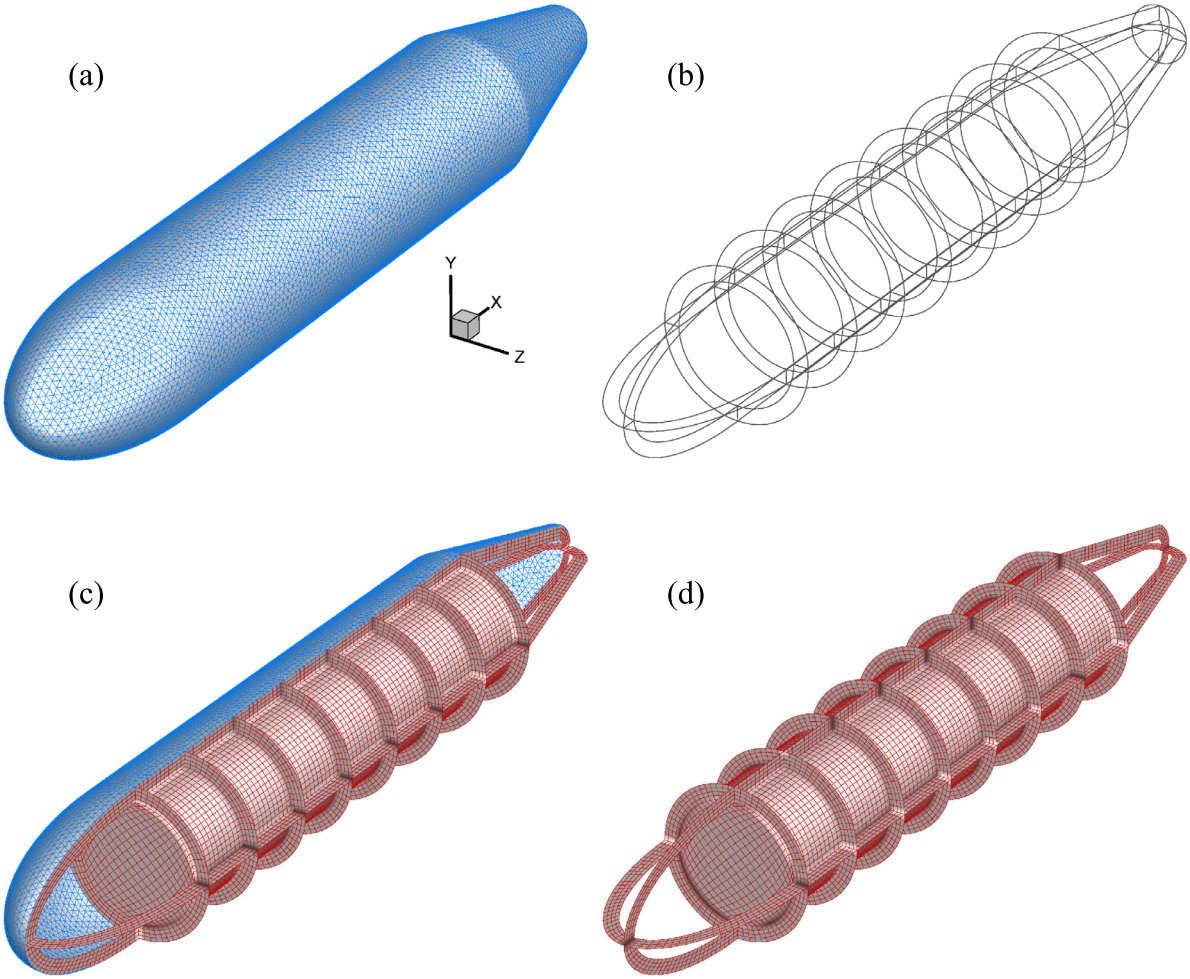

Fig. 6. Geometry of the model and its FE/BE meshes: (a) the outer hull; (b) the contour plot; (c) the cross-sectional view and (d) the internal structure.

length of 11.85 m and thus in the light of the Lagrange remainder, the suitable number of expansion terms required for a desired level of accuracy is $L = 35$ for this application case.

The use of the automatic reduction algorithm results in a ROM with merely 539 DOFs in which $n = 248$ for the reduced displacement DOFs and $m = 291$ for the reduced pressure DOFs, while using only three expansion points, i.e. $s_\star = \mathrm{j}ck_\star = 2\pi\mathrm{j} \times [175, 350, 550]$ with $\mathtt{lub} = 10^{10}$ and $4\hat{L} = 96$. It should be mentioned that the last expansion point $s_3 = \mathrm{j}ck_3 = 2\pi\mathrm{j} \times 550$ is outside the considered frequency range. This is because that in the first step only the structural loading without the unknown acoustic loading is included to construct the orthonormal basis $\mathbf{V}$. However, in the vibro-acoustic coupling system with heavy medium of water, the fluid which acts as an added mass can significantly decrease the natural frequencies of the pure structural system [52], which means that the additional dynamical information above 500 Hz should be contained in the proposed model order reduction process to take into account the contribution of higher-order modes in dynamical responses of the lower frequency range.

With the generated compact ROM of dimension $n+m = 539$, time-harmonic structural displacement and acoustic pressure fields caused by the input excitations at any position in their respective domains can be easily predicted. Since the dynamic behavior at loading locations is usually the output quantity of interest, the variations as a function of the frequency of the absolute values of displacements in the $+z$ direction at the points $(2, 0, -0.8)$ m and $(4, 0, -0.8)$ m are shown in Fig. 7. Considering computational resource limitations, the solution of the large-scale full-order model with 457094 DOFs is difficult to achieve. Therefore, for the purpose of comparison, an FE–BE

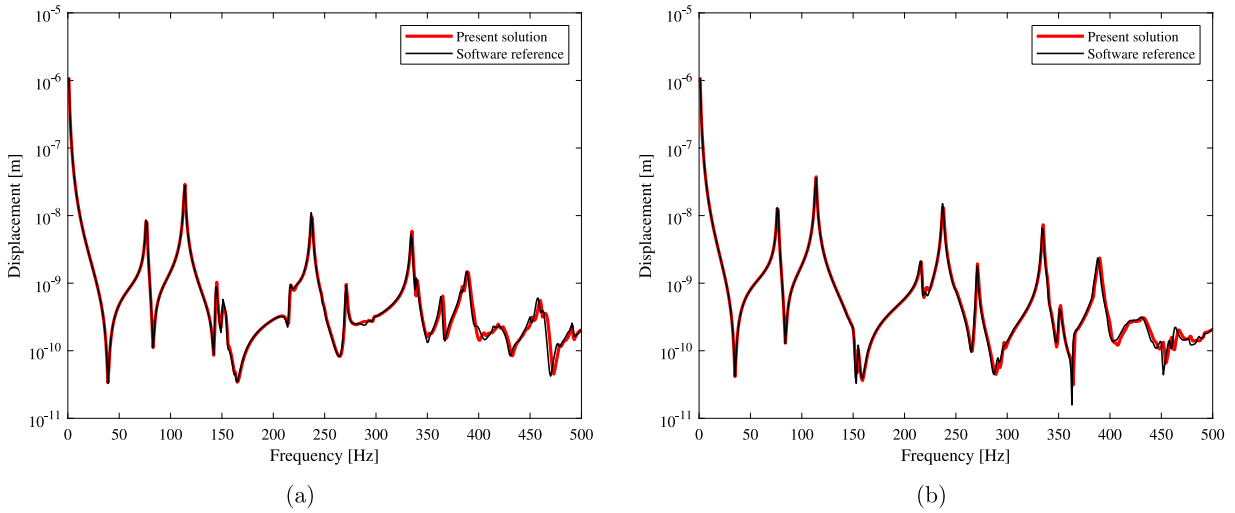

Fig. 7. Dynamical displacement responses at the points: (a) $(2, 0, -0.8)$ m; (b) $(4, 0, -0.8)$ m.

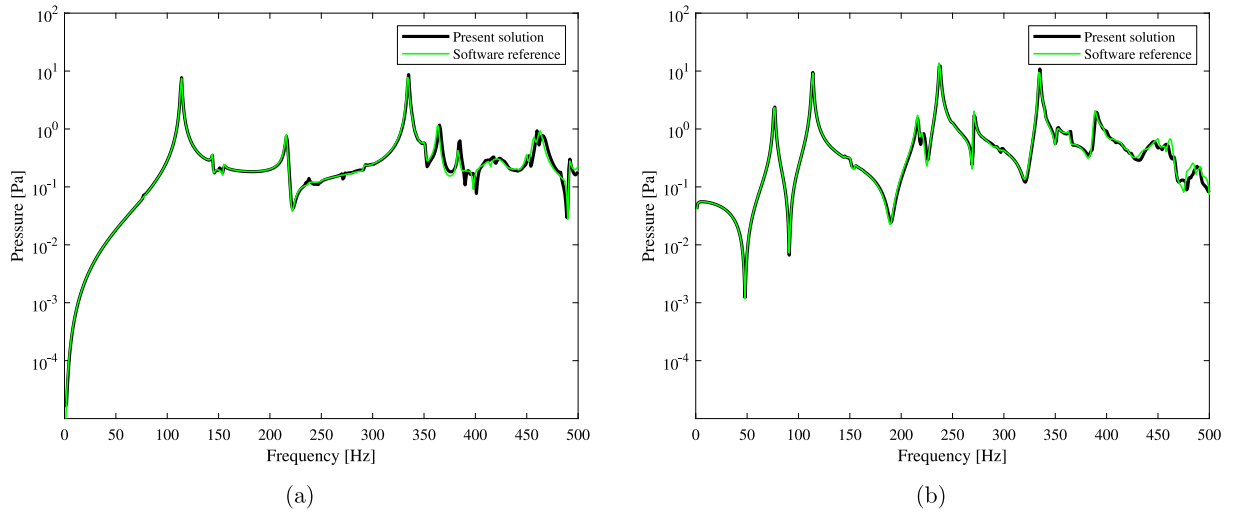

Fig. 8. Dynamical pressure responses at the points: (a) $(5, 1, 0)$ m; (b) $(4, 0, -1)$ m.

reference solution is sought in COMSOL, which has the same FE quadratic shell elements for the structure and yet linear/linear shape functions for the pressure/normal acceleration in the BE acoustic field, leading to a total of 458332 complex-valued DOFs. It is clear that the proposed three-step MOR solution procedure produces results very close to the software solution which confirms its high accuracy.

Fig. 8 reports the predicted acoustic pressure amplitude versus the frequency at coordinates $(5, 1, 0)$ m and $(4, 0, -1)$ m located on the outer-surface of the hull. Due to the lack of transfer functions obtained from the FOM, the solid green line again represents the solution from the commercial FE–BE solver COMSOL and serves as a reference. This clearly illustrates that the present approach yields rather accurate results for different field points within the acoustic domain. In order to better assess the computational accuracy of the proposed technique, an average prediction difference ϵ for the sound pressure at the response point is defined as:

$$\epsilon = \frac{1}{N_{freq}} \sum_{d=1}^{N_{freq}} \frac{|p^d - p^d_{\text{ref}}|}{|p^d_{\text{ref}}|} \tag{22}$$

where N_{freq} (= 500) is the number of discrete frequencies at which the pressure response function (p^d: present solutions; p^d_{ref}: numerical references calculated using COMSOL) is evaluated. In this case, the average value ϵ of 7% is seen, where the relative difference in the lower frequency region does not exceed 3%, whereas the relative difference in the upper frequency region becomes larger. However, the results are still acceptable as given in Fig. 8.

For this complicated case, the CPU time spent in constructing the two orthonormal bases $\mathbf{V}$ and $\mathbf{W}$ (the offline phase) is respectively 805 s and 9 h, whereas the execution time consumed by the online frequency-wise sweep analysis is 29 s, only taking up a very small percentage. Again, the largest proportion of the elapsed time happens in the offline phase (99.9%). The total processing time required to solve the frequency responses of the reference model via the commercial FE–BE solver equipped with the default GMRES and SAI is 27 h. The present approximation method proves about 2 times reduction in computational cost over the commercial software even though the same mesh discretization and (nearly) equal DOFs are used. Thus it is more efficient due to a lower number of DOFs, a faster simulation, meanwhile keeping almost the same accuracy in the entire frequency range of interest.

These results validate the strength and applicability of the presented MOR technique for strongly coupled exterior vibro-acoustic problems, both on the accuracy and the computational efficiency. We also emphasize that the program written in MATLAB is a proof of concept and is not yet exclusively optimized. Also, no effort is attempted to parallelize the algorithm. In this sense that a further substantial speed improvement can be achieved by converting ad-hoc MATLAB routines into a high performance programming language such as executable FORTRAN or C++ with efficient parallelization, which is currently being investigated intensively.

5. Conclusions

A novel three-step model order reduction technique is proposed in this paper for accelerating steady-state frequency response predictions of exterior structural–acoustic interaction systems, in which the hybrid FE–BE modeling technique is provided to flexibly couple constant acoustic BE models with higher order structural FE models. In order to avoid full-scale simulations and enable drastic reduction of the overall computational load, the specific shapes and essential properties (e.g., model size, bandwidth) of the physically diverse submatrices in the general dynamical equations are fully exploited. To this effect, with respect to the two different subsystems, different orders of Krylov subspaces are separately served as projection subspaces for dimension reduction. First, a second-order Arnoldi (SOAR) procedure is used to construct an orthonormal basis for large but sparse FE matrices, where Rayleigh damping is inserted. After omitting the reduced structural displacement DOFs from the global system of equations, the Krylov subspace-based (linear) first-order Arnoldi (FOAR) method is applied to the resulting expression to create another orthonormal basis for relatively small but dense BE pressure DOFs, in which the representative affine decomposition is introduced to facilitate the matrix assembly and to increase its robustness with respect to frequency changes. More specifically, the frequency-dependent integral kernels are decoupled into a finite sum of frequency-dependent scalar functions multiplied by frequency-independent terms. To the end, having two different projection matrices generated during the offline stage at hand, a final reduced order model which holds the same form and intrinsic dynamical features as the original full-order model can be quickly recovered by simple matrix operations and thus subsequent online evaluations based on the robust ROM at each frequency of interest are very cheap. Two case studies are examined which demonstrate that fast frequency sweep analyses with excellent speedups over the brute force approach and several times faster than the commercial software package can be achieved and the required computational resource in terms of both CPU time and memory consumption is very limited.

In view of efficient parametric studies arising from multi-query engineering applications, such as optimization design (size-, shape- and topology-optimization), parameter identification, uncertainty quantification of high-resolution vibro-acoustic systems, it would be worthwhile to further extend the present approach to the parametric model reduction framework, which allows to retain the (one or more) parameter-dependence in the low-dimensional yet accurate ROM.

Declaration of competing interest

The authors declare that they have no known competing financial interests or personal relationships that could have appeared to influence the work reported in this paper.

Acknowledgments

The authors would like to acknowledge the funding support from the National Natural Science Foundation of China (Grant Nos. 12002146 and 11972179). The research of X. Xie is also funded by the China Postdoctoral Science Foundation (Project Nos. 2020M672696 and 2021T140294) and the SUSTech Presidential Postdoctoral Fellowship. The authors gratefully acknowledge the anonymous reviewers for their constructive comments.

References

[1] O. Zienkiewicz, R. Taylor, J.Z. Zhu, The Finite Element Method: Its Basis and Fundamentals, Seventh, Elsevier Ltd, 2013, pp. 1–714, http://dx.doi.org/10.1016/C2009-0-24909-9.
[2] C.A. Brebbia, the Boundary Element Method for Engineers, Pentech Press, 1978, pp. 1–189.
[3] M.C. Junger, D. Feit, Sound, Structures, and their Interaction, MIT Press, Cambridge, 1972, pp. 1–470.
[4] G.C. Everstine, F.M. Henderson, Coupled finite element/boundary element approach for fluid-structure interaction, J. Acoust. Soc. Am. 87 (5) (1990) 1938–1947, http://dx.doi.org/10.1121/1.399320.
[5] S. Amini, P.J. Harris, D.T. Wilton, Coupled Boundary and Finite Element Methods for the Solution of the Dynamic Fluid-Structure Interaction Problem, Springer Berlin Heidelberg, 1992, pp. 1–94, http://dx.doi.org/10.1007/978-3-642-51727-3.
[6] Z.S. Chen, G. Hofstetter, H.A. Mang, A Galerkin-type BE-FE formulation for elasto-acoustic coupling, Comput. Methods Appl. Mech. Engrg. 152 (1–2) (1998) 147–155, http://dx.doi.org/10.1016/S0045-7825(97)00187-4.
[7] S.T. Christensen, S.V. Sorokin, N. Olhoff, On analysis and optimization in structural acoustics - part I: Problem formulation and solution techniques, Struct. Optim. 16 (2–3) (1998) 83–95, http://dx.doi.org/10.1007/bf01202818.
[8] M. Fischer, L. Gaul, Fast BEM-FEM mortar coupling for acoustic-structure interaction, Internat. J. Numer. Methods Engrg. 62 (12) (2005) 1677–1690, http://dx.doi.org/10.1002/nme.1242.
[9] D. Brunner, M. Junge, L. Gaul, A comparison of FE-BE coupling schemes for large-scale problems with fluid-structure interaction, Internat. J. Numer. Methods Engrg. 77 (5) (2009) 664–688, http://dx.doi.org/10.1002/nme.2412.
[10] H. Peters, S. Marburg, N. Kessissoglou, Structural-acoustic coupling on non-conforming meshes with quadratic shape functions, Internat. J. Numer. Methods Engrg. 91 (1) (2012) 27–38, http://dx.doi.org/10.1002/nme.4251.
[11] N. Atalla, F. Sgard, Finite Element and Boundary Methods in Structural Acoustics and Vibration, CRC Press, 2015, pp. 1–444, http://dx.doi.org/10.1201/b18366.
[12] C. Rajakumar, A. Ali, Boundary element-finite element coupled eigenanalysis of fluid-structure systems, Internat. J. Numer. Methods Engrg. 39 (10) (1996) 1625–1634.
[13] M. Junge, D. Brunner, L. Gaul, Solution of FE-BE coupled eigenvalue problems for the prediction of the vibro-acoustic behavior of ship-like structures, Internat. J. Numer. Methods Engrg. 87 (7) (2011) 664–676, http://dx.doi.org/10.1002/nme.3124.
[14] H. Peters, N. Kessissoglou, S. Marburg, Modal decomposition of exterior acoustic-structure interaction, J. Acoust. Soc. Am. 133 (5) (2013) 2668–2677, http://dx.doi.org/10.1121/1.4796114.
[15] A. Kimeswenger, O. Steinbach, G. Unger, Coupled finite and boundary element methods for fluid-solid interaction eigenvalue problems, SIAM J. Numer. Anal. 52 (5) (2014) 2400–2414, http://dx.doi.org/10.1137/13093755x.
[16] C.J. Zheng, C.X. Bi, C. Zhang, H.F. Gao, H.B. Chen, Free vibration analysis of elastic structures submerged in an infinite or semi-infinite fluid domain by means of a coupled FE-BE solver, J. Comput. Phys. 359 (2018) 183–198, http://dx.doi.org/10.1016/j.jcp.2018.01.018.
[17] S.K. Baydoun, S. Marburg, Investigation of radiation damping in sandwich structures using finite and boundary element methods and a nonlinear eigensolver, J. Acoust. Soc. Am. 147 (3) (2020) 2020–2034, http://dx.doi.org/10.1121/10.0000947.
[18] T. Liang, J. Wang, J. Xiao, L. Wen, Coupled BE-FE based vibroacoustic modal analysis and frequency sweep using a generalized resolvent sampling method, Comput. Methods Appl. Mech. Engrg. 345 (2019) 518–538, http://dx.doi.org/10.1016/j.cma.2018.09.038.
[19] H. Peters, N. Kessissoglou, S. Marburg, Modal decomposition of exterior acoustic-structure interaction problems with model order reduction, J. Acoust. Soc. Am. 135 (5) (2014) 2706–2717, http://dx.doi.org/10.1121/1.4869086.
[20] E.J. Grimme, Krylov projection methods for model reduction, in: Vasa (Ph.D. thesis), University of Illinois at Urbana-Champaign, 1997.
[21] Z. Bai, Krylov subspace techniques for reduced-order modeling of large-scale dynamical systems, Appl. Numer. Math. 43 (1–2) (2002) 9–44, http://dx.doi.org/10.1016/S0168-9274(02)00116-2.
[22] Z. Bai, Y. Su, SOAR: A second-order arnoldi method for the solution of the quadratic eigenvalue problem, SIAM J. Matrix Anal. Appl. 26 (3) (2005) 640–659, http://dx.doi.org/10.1137/S0895479803438523.
[23] Z. Bai, Y. Su, Dimension reduction of large-scale second-order dynamical systems via a second-order Arnoldi method, SIAM J. Sci. Comput. 26 (5) (2005) 1692–1709, http://dx.doi.org/10.1137/040605552.
[24] J.A. Giordano, G.H. Koopmann, State space boundary element-finite element coupling for fluid-structure interaction analysis, J. Acoust. Soc. Am. 98 (1) (1995) 363–372, http://dx.doi.org/10.1121/1.413691.
[25] A.C. Antoulas, Approximation of Large-Scale Dynamical Systems, Society for Industrial and Applied Mathematics, 2005, http://dx.doi.org/10.1137/1.9780898718713.
[26] U. Hetmaniuk, R. Tezaur, C. Farhat, Review and assessment of interpolatory model order reduction methods for frequency response structural dynamics and acoustics problems, Internat. J. Numer. Methods Engrg. 90 (13) (2012) 1636–1662, http://dx.doi.org/10.1002/nme.4271.
[27] B. Besselink, U. Tabak, A. Lutowska, N. Van De Wouw, H. Nijmeijer, D.J. Rixen, M.E. Hochstenbach, W.H. Schilders, A comparison of model reduction techniques from structural dynamics, numerical mathematics and systems and control, J. Sound Vib. 332 (19) (2013) 4403–4422, http://dx.doi.org/10.1016/j.jsv.2013.03.025.

[28] J.P. Tuck-Lee, P.M. Pinsky, Adaptive frequency windowing for multifrequency solutions in structural acoustics based on the matrix Padé-via-Lanczos algorithm, Internat. J. Numer. Methods Engrg. 73 (5) (2008) 728–746, http://dx.doi.org/10.1002/nme.2102.
[29] U. Hetmaniuk, R. Tezaur, C. Farhat, An adaptive scheme for a class of interpolatory model reduction methods for frequency response problems, Internat. J. Numer. Methods Engrg. 93 (10) (2013) 1109–1124, http://dx.doi.org/10.1002/nme.4436.
[30] R. Srinivasan Puri, D. Morrey, A.J. Bell, J.F. Durodola, E.B. Rudnyi, J.G. Korvink, Reduced order fully coupled structural-acoustic analysis via implicit moment matching, Appl. Math. Model. 33 (11) (2009) 4097–4119, http://dx.doi.org/10.1016/j.apm.2009.02.016.
[31] X. Xie, H. Zheng, S. Jonckheere, A. van de Walle, B. Pluymers, W. Desmet, Adaptive model reduction technique for large-scale dynamical systems with frequency-dependent damping, Comput. Methods Appl. Mech. Engrg. 332 (2018) 363–381, http://dx.doi.org/10.1016/j.cma.2017.12.023.
[32] X. Xie, H. Zheng, S. Jonckheere, B. Pluymers, W. Desmet, A parametric model order reduction technique for inverse viscoelastic material identification, Comput. Struct. 212 (2019) 188–198, http://dx.doi.org/10.1016/j.compstruc.2018.10.013.
[33] Y.J. Liu, Fast Multipole Boundary Element Method: Theory and Applications in Engineering, Cambridge University Press, 2009, pp. 1–235, http://dx.doi.org/10.1017/CBO9780511605345.
[34] S. Schneider, FE/FMBE coupling to model fluid-structure interaction, Internat. J. Numer. Methods Engrg. 76 (13) (2008) 2137–2156, http://dx.doi.org/10.1002/nme.2399.
[35] D. Brunner, G. Of, M. Junge, O. Steinbach, L. Gaul, A fast BE-FE coupling scheme for partly immersed bodies, Internat. J. Numer. Methods Engrg. 81 (1) (2010) 28–47, http://dx.doi.org/10.1002/nme.2672.
[36] L. Chen, C. Zheng, H. Chen, FEM/wideband FMBEM coupling for structural-acoustic design sensitivity analysis, Comput. Methods Appl. Mech. Engrg. 276 (2014) 1–19, http://dx.doi.org/10.1016/j.cma.2014.03.016.
[37] Y. Saad, M.H. Schultz, GMRES: A generalized minimal residual algorithm for solving nonsymmetric linear systems, SIAM J. Sci. Stat. Comput. 7 (3) (1986) 856–869, http://dx.doi.org/10.1137/0907058.
[38] P. Avery, C. Farhat, G. Reese, Fast frequency sweep computations using a multi-point Padé-based reconstruction method and an efficient iterative solver, Internat. J. Numer. Methods Engrg. 69 (13) (2007) 2848–2875, http://dx.doi.org/10.1002/nme.1879.
[39] J.-P. Coyette, C. Lecomte, J.-L. Migeot, J. Blanche, M. Rochette, G. Mirkovic, Calculation of vibro-acoustic frequency response functions using a single frequency boundary element solution and a Padé expansion, Acta Acust. United Acust. 85 (3) (1999) 371–377, https://eprints.soton.ac.uk/342607/.
[40] M. Malhotra, P.M. Pinsky, Efficient computation of multi-frequency far-field solutions of the Helmholtz equation using Padé approximation, J. Comput. Acoustics 8 (1) (2000) 223–240, http://dx.doi.org/10.1142/S0218396X00000145.
[41] X. Xie, Y.J. Liu, An adaptive model order reduction method for boundary element-based multi-frequency acoustic wave problems, Comput. Methods Appl. Mech. Engrg. 373 (2021) 113532, http://dx.doi.org/10.1016/j.cma.2020.113532.
[42] S.K. Baydoun, M. Voigt, C. Jelich, S. Marburg, A greedy reduced basis scheme for multifrequency solution of structural acoustic systems, Internat. J. Numer. Methods Engrg. 121 (2) (2020) 187–200, http://dx.doi.org/10.1002/nme.6205.
[43] Y.J. Liu, On the BEM for acoustic wave problems, Eng. Anal. Bound. Elem. 107 (2019) 53–62, http://dx.doi.org/10.1016/j.enganabound.2019.07.002.
[44] Z. Liu, M. Majeed, F. Cirak, R. N. Simpson, Isogeometric FEM-BEM coupled structural-acoustic analysis of shells using subdivision surfaces, Internat. J. Numer. Methods Engrg. 113 (9) (2018) 1507–1530, http://dx.doi.org/10.1002/nme.5708.
[45] F. Cuvelier, C. Japhet, G. Scarella, An efficient way to assemble finite element matrices in vector languages, BIT Numer. Math. 56 (3) (2016) 833–864, http://dx.doi.org/10.1007/s10543-015-0587-4, arXiv:1401.3301.
[46] X. Xie, H. Zheng, S. Jonckheere, W. Desmet, Acoustic simulation of cavities with porous materials using an adaptive model order reduction technique, J. Sound Vib. 485 (2020) 115570, http://dx.doi.org/10.1016/j.jsv.2020.115570.
[47] S. Li, An efficient technique for multi-frequency acoustic analysis by boundary element method, J. Sound Vib. 283 (3–5) (2005) 971–980, http://dx.doi.org/10.1016/j.jsv.2004.05.027.
[48] Z. Wang, Z.G. Zhao, Z.X. Liu, Q.B. Huang, A method for multi-frequency calculation of boundary integral equation in acoustics based on series expansion, Appl. Acoust. 70 (3) (2009) 459–468, http://dx.doi.org/10.1016/j.apacoust.2008.05.005.
[49] A.J. Burton, G.F. Miller, The application of integral equation methods to the numerical solution of some exterior boundary-value problems, Proc. R. Soc. Lond. Ser. A Math. Phys. Eng. Sci. 323 (1553) (1971) 201–210, http://dx.doi.org/10.1098/rspa.1971.0097.
[50] D. Lu, Y. Su, Z. Bai, Stability analysis of the two-level orthogonal Arnoldi procedure, SIAM J. Matrix Anal. Appl. 37 (1) (2016) 195–214, http://dx.doi.org/10.1137/151005142.
[51] COMSOL Multiphysics. http://www.comsol.com/livelink-for-matlab.
[52] X. Xie, H. Zheng, Y. Qu, A variational formulation for vibro-acoustic analysis of a panel backed by an irregularly-bounded cavity, J. Sound Vib. 373 (2016) 147–163, http://dx.doi.org/10.1016/j.jsv.2016.03.003.